

Optimizing Binary Decision Diagrams with MaxSAT for classification*

Hao Hu, Marie-José Huguet, Mohamed Siala

LAAS-CNRS, Université de Toulouse, CNRS, INSA, Toulouse, France
{hhu, huguet, siala}@laas.fr

Abstract

The growing interest in explainable artificial intelligence (XAI) for critical decision making motivates the need for interpretable machine learning (ML) models. In fact, due to their structure (especially with small sizes), these models are inherently understandable by humans. Recently, several exact methods for computing such models are proposed to overcome weaknesses of traditional heuristic methods by providing more compact models or better prediction quality.

Despite their compressed representation of Boolean functions, Binary decision diagrams (BDDs) did not gain enough interest as other interpretable ML models. In this paper, we first propose SAT-based models for learning optimal BDDs (in terms of the number of features) that classify all input examples. Then, we lift the encoding to a MaxSAT model to learn optimal BDDs in limited depths, that maximize the number of examples correctly classified. Finally, we tackle the fragmentation problem by introducing a method to merge compatible subtrees for the BDDs found via the MaxSAT model. Our empirical study shows clear benefits of the proposed approach in terms of prediction quality and interpretability (i.e., lighter size) compared to the state-of-the-art approaches.

1 Introduction

Due to the increasing concerns in understanding the reasoning behind AI decisions for critical applications, interpretable Machine Learning (ML) models gained a lot of attention. Examples of such ML applications include job recruitment, bank credit applications, and justice (Voigt and Bussche 2017). Most of traditional approaches for building interpretable models are greedy, for example, decision trees (Breiman et al. 1984; Quinlan 1986, 1993), rule lists (Cohen 1995; Clark and Boswell 1991), and decision sets (Lakkaraju, Bach, and Leskovec 2016). Compared to traditional approaches, exact methods offer guarantee of optimality, such as model size and accuracy. In this context, combinatorial optimisation methods, such as Constraint Programming (Bonfietti, Lombardi, and Milano 2015; Verhaeghe et al. 2020), Mixed Integer Programming (Angelino et al. 2018; Verwer and Zhang 2019; Aglin, Nijssen, and Schaus 2020), or Boolean Satisfiability (SAT) (Bessiere,

Hebrard, and O’Sullivan 2009; Narodytska et al. 2018; Avelaneda 2020; Hu et al. 2020; Janota and Morgado 2020; Yu et al. 2020) have been successfully used to learn interpretable models. These declarative approaches are particularly interesting since they offer certain flexibility to handle additional requirements when learning a model.

Decision Trees are widely used as a standard interpretable model. However, they suffer from two major flaws: *replication* and *fragmentation* (Matheus and Rendell 1989; Pagallo and Haussler 1990; Rokach and Maimon 2014). The *replication* problem appears when two identical subtrees are in the decision tree. The *fragmentation* problem appears when only few samples are associated to leaf nodes. By providing compact representations for Boolean functions, Binary Decision Diagrams (BDDs) (Akers 1978; Moret 1982; Bryant 1986; Knuth 2009) are widely studied for hardware design, model checking, and knowledge representation. In the context of ML, BDD could be viewed as an interpretable model for binary classification. In addition, they were extended for multi-classification, known as *decision graphs* and heuristic methods were proposed in (Oliver 1993; Kohavi 1994; Kohavi and Li 1995; Mues et al. 2004). Moreover, (Ignatov and Ignatov 2017) proposed *decision stream*, a similar topology to BDD based on merging *similar* subtrees in each split made in decision trees to improve the generalization. (Oliver 1993; Kohavi 1994) showed that *decision graphs* could avoid the *replication* problem and *fragmentation* problem of decision trees effectively. For binary classification, BDDs also could avoid these problems. This fact indicates that generally in the practice of ML, a BDD have a smaller size than the corresponding decision tree.

In this paper, we introduce a SAT-based model for learning optimal BDDs with the smallest number of features classifying all examples correctly, and a lifted MaxSAT-based model to learn optimal BDDs minimizing the classification error. We assume that all BDDs are *ordered* and *reduced*¹, the limitation on the depth for a BDD, corresponds to the number of features to be selected by our model. To the best of our knowledge, (Cabodi et al. 2021) is the only exact method of learning optimal BDDs in the context of ML. The authors proposed a SAT model to learn optimal BDDs with the smallest sizes that correctly classify all examples. In their

*This is the preprint version of the paper (Hu, Huguet, and Siala 2022)

¹The two notions are defined in the background

approach, the depth of the BDD is not restrained. In fact, it is possible that the constructed BDD is small in size (number of nodes) and high in depth. As the BDD is *ordered*, this approach could not limit the number of features used, making it not quite comparable with our proposition. Another related work is in (Hu et al. 2020) where the authors consider a MaxSAT model to learn optimal decision trees minimizing the classification error within a limited depth. The usage of the same solving methodology with the same objective function and the depth limit, makes these two MaxSAT models comparable. Finally, in order to increase the scalability of our approach, we propose a heuristic extension based on a simple pre-processing step.

The rest of the paper is organized as follows. First, we give the related technical background in Section 2. Then, in Section 3, we show the proposed SAT and MaxSAT models for learning BDDs in binary classification. Finally in Section 4, we present our large experimental studies to show the competitive prediction quality of the proposed approach.

2 Technical Background

Classification

Consider a dataset $\mathcal{E} = \{e_q, \dots, e_M\}$ with M examples. Each example $e_q \in \mathcal{E}$ is characterized by a list of binary features $\mathcal{L}_q = [f_1, \dots, f_K]$ and a binary target cl_q , representing the class of the example ($cl_q \in \{0, 1\}$). The data set is partitioned into \mathcal{E}^+ and \mathcal{E}^- , where \mathcal{E}^+ (respectfully \mathcal{E}^-) is the set of positive (respectfully negative) examples. That is, $cl_q = 1$ iff $e_q \in \mathcal{E}^+$ and $cl_q = 0$ iff $e_q \in \mathcal{E}^-$. We assume that, $\forall 1 \leq q, q' \leq M$, $\mathcal{L}_q = \mathcal{L}_{q'}$ implies $cl_q = cl_{q'}$.

Let ϕ be the function defined by $\phi(\mathcal{L}_q) = cl_q$, $\forall q \in [1, M]$. The classification problem is to compute a function γ (called a *classifier*) that matches as accurately as possible the function ϕ on examples e_q of the training data and generalizes well on unseen test data.

Binary Decision Diagrams

Binary Decision Diagrams (BDDs) are used to provide compact representation of Boolean functions. Let $[x_1, \dots, x_n]$ be a sequence of n Boolean variables. A BDD is a rooted, directed, acyclic graph \mathcal{G} . The vertex set \mathcal{V} of \mathcal{G} contains two types of vertices. A *terminal* vertex v is associated to a binary value: $value(v) \in \{0, 1\}$. A *nonterminal* vertex v , is associated to a Boolean variable x_i and has two children $left(v), right(v) \in \mathcal{V}$. In this case, $index(v) = i \in \{1, \dots, n\}$ is the index of the Boolean variable associated to v .

We assume that all BDDs are *ordered* and *reduced*. These two restrictions are widely considered in the literature as they guarantee a *unique* BDD for a given Boolean function. The restriction *ordered* indicates that for any *non-terminal* vertex v , $index(v) < index(left(v))$ and $index(v) < index(right(v))$. The restriction *reduced* indicates that the graph contains no *nonterminal* vertex v with $left(v) = right(v)$, nor does it contain distinct *nonterminal* vertices v and v' having isomorphic rooted sub-graphs. Therefore, given an *ordered reduced* BDD \mathcal{G} with *root* v , the associated Boolean function can be recursively obtained with the Shannon expansion process (Shannon 1938).

Let g be a Boolean function defined over a sequence $\mathcal{X} = [x_1, \dots, x_n]$ of n Boolean variables. The function g can be represented by a *truth table* that lists the 2^n values of all assignments of the n variables. The value of the truth table is therefore associated to a string of 2^n binary values. A truth table β of length 2^n is said to be of order n . A truth table β of order $n > 0$ has the form $\beta_0\beta_1$, where β_0 and β_1 are truth tables of order $n - 1$, and β_0 and β_1 are called *subtables* of β . The *subtables* of *subtables* are also considered to be *subtables*, and a table is considered as a *subtable* of itself. A *bead* of order n is a truth table T of order n that does not have the form $\alpha\alpha$ where α is a subtable of T . The *beads* of g are the *subtables* of its truth table that happen to be *beads*. Proposition 1 from (Knuth 2009) relates truth table and binary decision diagram for the same Boolean function.

Proposition 1. *All vertices in \mathcal{V} of a binary decision diagram \mathcal{G} , are in one-to-one correspondence with the beads of the Boolean function g it represents.*

Based on Proposition 1, we can produce the ordered and reduced binary decision diagram of a Boolean function by finding its *beads* and combine its *beads* with its sequence of variables. An algorithm for producing the corresponding BDD is provided in the Appendix.

Example 1. *Consider the Boolean function from (Knuth 2009): $g_1(x_1, x_2, x_3) = (x_1 \vee x_2) \wedge (x_2 \vee x_3) \wedge (x_1 \vee x_3)$. The binary string associated to its truth table β is 00010111. The beads of β are $\{00010111, 0001, 0111, 01, 0, 1\}$.*

From Proposition 1, we can draw the BDD with the beads found, shown as the left part of Figure 1. The dashed (solid) line of each vertex indicates the left (right) child. Then, we can replace the beads by vertices associated with the sequence of Boolean variables. The final binary decision diagram for g_1 is shown as the right part of Figure 1.

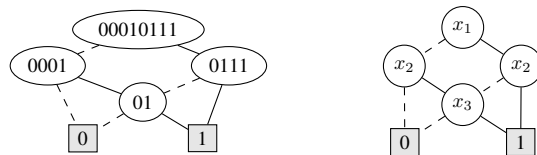


Figure 1: The Binary decision diagram for $g_1(x_1, x_2, x_3)$

Oblivious Read-Once Decision Graphs

Oblivious Read-Once Decision Graphs (OODGs) are proposed in (Kohavi 1994) to overcome some limitations of decision trees for multi-classification, like *replication* and *fragmentation* problem. We refer the readers to (Kohavi and Li 1995; Kohavi 1994) for details on OODGs. An OODG is a rooted, directed, acyclic graph, which contains terminal *category nodes* labelled with classes to make decisions, and non-terminal *branching nodes* labelled with features to make splits. The property “*read-once*” indicates that each feature occurs at most once along any path from the root to a category node. The property “*levelled*” indicates that the nodes are partitioned into a sequence of pairwise disjoint sets, representing the levels, such that outgoing edges from

each level terminate at the next level. The property “*oblivious*” extends the idea of “*levelled*” by guaranteeing that all nodes at a given level are labelled by the same feature.

For the classification process, top-down and bottom-up heuristic methods for building OODGs are proposed in (Kohavi and Li 1995; Kohavi 1994). Here, we introduce briefly the top-down heuristic method, which is similar to the heuristic methods C4.5 and CART for computing decision trees. The top-down heuristic induction for OODG with given depth contains three critical phases: (1) selecting a sequence of features with the help of *mutual information* (the difference of *conditional entropy* (Cover and Thomas 2006)); (2) growing an oblivious decision tree (ODT) by splitting the dataset with features in the sequence selected; and (3) merging *isomorphic* and *compatible* subtrees from top to down to build the OODG. When building the ODT, the algorithm marks nodes that capture no example of the dataset as “*unknown*”. For the merging phase, two subtrees are *compatible* if at least one root is labelled as “*unknown*”, or if the two root nodes are labelled with same feature and their corresponding children are the roots of compatible subtrees. The ODT grown could make classifications directly by assigning “*unknown*” nodes with the majority class of their parents.

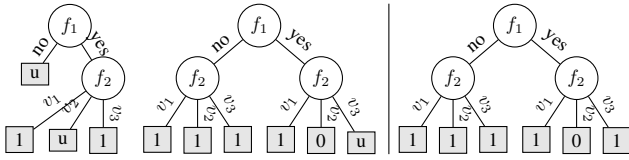


Figure 2: An example of two compatible subtrees (the left two) and the merged tree (the right one) from (Kohavi and Li 1995)

Figure 2 shows an example of two compatible subtrees and the merged tree, where “*unknown*” nodes are labelled as “*u*”. Merging compatible subtrees changes the bias by assuming that a “*unknown*” node is likely to behave the same as another child if they belong to compatible subtrees.

In binary classification for binary datasets, OODGs could be considered *equivalent* to BDDs, as the properties “*oblivious*” and “*read-once*” for OODGs are same as property “*ordered*” for BDDs. In addition, the use of merging compatible subtrees could also be applied for BDDs.

SAT & MaxSAT

We use standard terminology for Boolean Satisfiability (Biere et al. 2009). A *literal* is a Boolean variable or its negation, and a *clause* is a disjunction of literals. An assignment of variables satisfies a clause if one of its literals is true. Given a set of Boolean variables and a set of clauses defined over these variables, the SAT problem can be defined as finding an assignment of the variables such that all the clauses are satisfied. Maximum Satisfiability (MaxSAT) is an optimization version of the SAT problem, where the clauses are partitioned into *hard* and *soft* clauses. Here we consider the Partial MaxSAT problem, that is to find an assignment of the Boolean variables that satisfies all the hard clauses and maximizes the number of satisfied soft clauses.

3 (Max)SAT-based model for Binary Decision Diagrams

In this section, we present our approach for learning BDDs for binary classification using SAT and MaxSAT.

Problem Definition

We firstly consider the following decision problem for classification with BDD in a given depth.

- $P_{bdd}(\mathcal{E}, H)$: Given a set of examples \mathcal{E} , is there a BDD of depth H that classifies correctly all examples in \mathcal{E} ?

Notice that the algorithm for $P_{bdd}(\mathcal{E}, H)$ can be used to the alternative problem of optimizing a BDD that classifies all examples in the dataset correctly with a minimum depth. For that purpose, one can use a linear search that takes an initial depth H_0 as input and progressively increases or decreases this value depending on the result of solving $P_{bdd}(\mathcal{E}, H)$.

Next, we consider another optimization problem for the classification with BDD in a limited depth.

- $P_{bdd}^*(\mathcal{E}, H)$: Given a set of examples \mathcal{E} , find a BDD of depth H that maximises the number of examples in \mathcal{E} that are correctly classified.

We propose an initial SAT model for the decision problem $P_{bdd}(\mathcal{E}, H)$. Then, we propose an improved version in tighter formula size. Finally, we show how the improved SAT model for $P_{bdd}(\mathcal{E}, H)$ can be used effectively to solve the optimization problem $P_{bdd}^*(\mathcal{E}, H)$ with MaxSAT.

SAT Model for $P_{bdd}(\mathcal{E}, H)$

As shown in Section 2, a BDD of depth H could be generated from the combination of a sequence of Boolean variables of size H : $[x_1, \dots, x_H]$, and a truth table of order H associated to a Boolean function. To solve the classification problem $P_{bdd}(\mathcal{E}, H)$, we then have to find a sequence of binary features of size H that maps one-to-one the sequence of Boolean variables, and a truth table associated to a Boolean function that well-classified all examples. We denote the sequence of binary features found as *feature ordering*. Therefore, the SAT encoding consists of two parts:

- **Part 1:** Constraints for selecting features of the dataset into the feature ordering of size H .
- **Part 2:** Constraints for generating a truth table that classifies all examples of \mathcal{E} correctly with the selected feature ordering.

To realize the SAT encoding, we introduce two sets of Boolean variables as follow:

- a_r^i : the variable a_r^i is 1 iff feature f_r is selected as i -th feature in the feature ordering, where $i = 1, \dots, H$, $r = 1, \dots, K$.
- c_j : the variable c_j is 1 iff the j -th value of the truth table is 1, where $j = 1, \dots, 2^H$.

The set of variables a_r^i guarantees the *ordered* restriction. Then, we introduce two constraints (1) and (2) for the feature ordering. Constraint 1 ensures that any feature f_r can

be selected at most once.

$$\sum_{i=1}^H a_r^i \leq 1, \quad r = 1, \dots, K \quad (1)$$

Then, there is exactly one feature selected for each index of the feature ordering.

$$\sum_{r=1}^K a_r^i = 1, \quad i = 1, \dots, H \quad (2)$$

We use the classical sequential counter encoding proposed in (Sinz 2005) to model constraints (1) and (2) as a Boolean formula.

The truth table we are looking for is the binary string of the values of variables $c_1 c_2 \dots c_{2^H}$. To avoid the first feature selected makes useless split, we need to make sure that the truth table is a *bead*.

$$\bigvee_{j=1}^{2^{H-1}} (c_j \oplus c_{j+2^{H-1}}) \quad (3)$$

There is a relationship between the values of a truth table and the assignments of the given sequence of Boolean variables. For example, the first value of a truth table corresponds to the assignment that $x_1 = 0$ and $x_2 = 0$. Therefore, we define the following function to obtain the value of the i -th feature in the feature ordering of size H given the j -th value in the truth table.

$$rel(i, j) = \lfloor \frac{j-1}{2^{H-i}} \rfloor \bmod 2, \quad i \in [1, H], j \in [1, 2^H] \quad (4)$$

For an example $e_q \in \mathcal{E}$, we denote the value of the feature f_r as $\sigma(r, q)$. If $rel(i, j) = \sigma(r, q)$, it indicates that for example e_q , the feature f_r can be at the i -th position in the feature ordering to produce the j -th value in the truth table. To classify all examples correctly, we ensure that no example follows an assignment in the truth table leading to its opposite class. Thus, we propose the following constraints for classification. Let $e_q \in \mathcal{E}^+$, for all $j = 1, \dots, 2^H$:

$$\neg c_j \rightarrow \bigvee_{i=1}^H \bigvee_{r=1}^K (a_r^i \wedge rel(i, j) \oplus \sigma(r, q)) \quad (5)$$

That is, for every positive example e_q , any variable c_j assigned to 0 must be associated to an assignment of features that contains at least one feature-value that is not coherent with e_q . For negative examples, we use a similar idea. Let $e_q \in \mathcal{E}^-$, for all $j = 1, \dots, 2^H$:

$$c_j \rightarrow \bigvee_{i=1}^H \bigvee_{r=1}^K (a_r^i \wedge rel(i, j) \oplus \sigma(r, q)) \quad (6)$$

Example 2. Let \mathcal{E}_0 be the given set of examples shown in Table 1. Figure 3 shows the corresponding decision tree classifying all examples correctly. We consider to encode a BDD with depth $H = 2$ classifying all examples of \mathcal{E}_0 correctly.

\mathcal{E}_0	f_1	f_2	f_3	f_4	label
e_1	1	0	1	0	0
e_2	1	0	0	1	0
e_3	0	0	1	0	1
e_4	1	1	0	0	0
e_5	0	0	0	1	1
e_6	1	1	1	1	0
e_7	0	1	1	0	0
e_8	0	0	1	1	1

Table 1: A dataset for binary classification

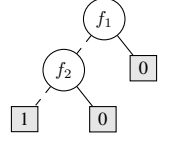


Figure 3: Decision Tree found

The two sets of variables are: $\{a_1^1, a_2^1, a_3^1, a_4^1, a_1^2, a_2^2, a_3^2, a_4^2\}$, and $\{c_1, c_2, c_3, c_4\}$. The constraints 1, 2, and 3 are:

$$\begin{aligned} a_1^1 + a_2^1 &\leq 1, & a_2^1 + a_3^1 &\leq 1, & a_3^1 + a_4^1 &\leq 1, & a_1^2 + a_2^2 &\leq 1, \\ a_1^1 + a_2^1 + a_3^1 + a_4^1 &= 1, & a_1^2 + a_2^2 + a_3^2 + a_4^2 &= 1 \\ & & (c_1 \oplus c_3) \vee (c_2 \oplus c_4) & & & & & \end{aligned}$$

For classification constraints (i.e., 5 and 6), we show the encoding of $e_1 \in \mathcal{E}^-$ with for value c_1 . The encoding for other examples and other values is similar.

$$\begin{aligned} c_1 \rightarrow & (a_1^1 \wedge 0 \oplus 1) \vee (a_2^1 \wedge 0 \oplus 0) \vee (a_3^1 \wedge 0 \oplus 1) \\ & \vee (a_4^1 \wedge 0 \oplus 0) \vee (a_1^2 \wedge 0 \oplus 1) \vee (a_2^2 \wedge 0 \oplus 0) \\ & \vee (a_3^2 \wedge 0 \oplus 1) \vee (a_4^2 \wedge 0 \oplus 0) \end{aligned}$$

This could be simplified as follow:

$$\neg c_1 \vee a_1^1 \vee a_3^1 \vee a_1^2 \vee a_3^2$$

$x_1 = f_1$	$x_2 = f_2$	
0	0	$c_1 = 1$
0	1	$c_2 = 0$
1	0	$c_3 = 0$
1	1	$c_4 = 0$

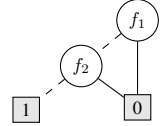


Table 2: Truth table solution for BDD of depth 2 classifying all example of \mathcal{E}_0 Figure 4: The BDD found

The values of truth table found by the SAT model are shown in Table 2, the feature ordering is $[f_1, f_2]$. Moreover, Table 2 illustrates the relationship between the values of truth table and the assignments of the given sequence Boolean variable of size 2. Figure 4 shows the corresponding BDD. This BDD classifies all examples of the dataset \mathcal{E}_0 correctly, also provides more compact representation than the decision tree shown in Figure 3.

We refer to this first SAT encoding for $P_{bdd}(\mathcal{E}, H)$ as BDD1. The size of BDD1 is given in Proposition 2.

Proposition 2. For a $P_{bdd}(\mathcal{E}, H)$ problem with K binary features and M examples, the encoding size (in terms of the number of literals used in the different clauses) of BDD1 is $O(M \times H \times K \times 2^H)$.

Proof. Notice first that j ranges from 1 to 2^H , i ranges from 1 to H , and r ranges from 1 to K . The term $M \times 2^H$ results from constraint (5) and (6), each contains $O(H \times K)$ literals. For the remaining constraints, it is $O(H \times K)$ for constraints (1) and (2), $O(2^H)$ for constraint (3). \square

The size of BDD1 is quite huge due to the size of clauses generated by constraints (5) and (6) for classification. This makes BDD1 impractical in practice.

An improved SAT Model for $P_{bdd}(\mathcal{E}, H)$

In order to reduce the size of BDD1, we propose new classification constraints to replace constraints (5) and (6). The idea is that every positive (respectively negative) example follows an assignment leading to a positive (respectively negative) value of the truth table. We introduce a new set of Boolean variables:

- d_i^q : The variable d_i^q is 1 iff for example e_q the value of the i -th feature selected in feature ordering is 1, where $i = 1, \dots, H, q = 1, \dots, M$.

Then, We describe constraints that relate the values of features for each example $e_q \in \mathcal{E}$, for $i = 1, \dots, H, r = 1, \dots, K$:

$$\begin{aligned} a_r^i &\rightarrow d_i^q & \text{if } \sigma(q, r) = 1 \\ a_r^i &\rightarrow \neg d_i^q & \text{if } \sigma(q, r) = 0 \end{aligned} \quad (7)$$

Let $e_q \in \mathcal{E}^+$, we have 2^H constraints for classifying examples correctly:

$$\begin{aligned} \neg d_1^q \wedge \neg d_2^q \wedge \dots \wedge \neg d_{H-1}^q \wedge \neg d_H^q &\rightarrow c_1 \\ \neg d_1^q \wedge \neg d_2^q \wedge \dots \wedge \neg d_{H-1}^q \wedge d_H^q &\rightarrow c_2 \\ &\dots \\ d_1^q \wedge d_2^q \wedge \dots \wedge d_{H-1}^q \wedge d_H^q &\rightarrow c_{2^H} \end{aligned} \quad (8)$$

That is, any positive example follows an assignment of the feature ordering that leads to a positive value in the truth table.

Similarly, for any $e_q \in \mathcal{E}^-$, we also have 2^H constraints:

$$\begin{aligned} \neg d_1^q \wedge \neg d_2^q \wedge \dots \wedge \neg d_{H-1}^q \wedge \neg d_H^q &\rightarrow \neg c_1 \\ \neg d_1^q \wedge \neg d_2^q \wedge \dots \wedge \neg d_{H-1}^q \wedge d_H^q &\rightarrow \neg c_2 \\ &\dots \\ d_1^q \wedge d_2^q \wedge \dots \wedge d_{H-1}^q \wedge d_H^q &\rightarrow \neg c_{2^H} \end{aligned} \quad (9)$$

We refer to this new SAT encoding for $P_{bdd}(\mathcal{E}, H)$ as BDD2. The encoding size of BDD2 is given in Proposition 3.

Proposition 3. For a $P_{bdd}(\mathcal{E}, H)$ problem with K binary features and M examples, the encoding size of the SAT encoding (BDD2) is $O(M \times H \times (2^H + K))$.

Proof. The term $M \times H \times K$ results from constraint (7). For constraints (8) and (9), for each example, there are 2^H clauses containing $H + 1$ literals. The term $M \times H \times 2^H$ results from that. \square

Propositions 2 and 3 show a clear theoretical advantage of BDD2 compared to BDD1 in terms of the encoding size, thus scalability.

MaxSAT Model for $P_{bdd}^*(\mathcal{E}, H)$:

We now present a MaxSAT encoding for the optimization problem $P_{bdd}^*(\mathcal{E}, H)$. That is, given a set of examples \mathcal{E} , find a binary decision diagram of depth H that maximises the number of examples correctly classified.

We transform the SAT encoding of BDDs into a MaxSAT encoding following a simple technique. The idea is to keep

structural constraints as hard clauses and classification constraints as soft clauses. We consider BDD2 as it has a reduced size. Constraints (1), (2), (3) and (7) are kept as hard clauses. To classify the examples, we declare all clauses of constraints (8) and (9) as soft clauses. For any example e_q , the number of satisfied soft clauses associated to e_q is either 2^H (indicating e_q is classified correctly), or $2^H - 1$ (indicating e_q is classified wrongly). Therefore, the objective of maximising the number of satisfied soft clauses is equivalent to maximise the number of examples correctly classified.

Merging Compatible Subtrees

Consider a BDD \mathcal{G} found by a MaxSAT solver and its associated truth table β . Based on the feature ordering of \mathcal{G} , it is possible that some values in β capture no (training) example (Equivalent to “unknown” nodes for OODG). Such values are decided by the MaxSAT solver in an arbitrary way, which gives a certain bias in generalisation. We propose to merge compatible subtrees in \mathcal{G} in order to handle this bias. This will result in changing some values in the truth table β (i.e. the arbitrary ones decided by MaxSAT).

We propose a post-processing procedure to merge compatible subtrees using the following three phase: (1) update the truth table β by replacing the values of β that capture no examples with a special value “u”; (2) for each level, check the beads, where “u” can be used to match 1 or 0, and create a node for each bead; (3) for each level, after creating the nodes, check the matches between all subtables of the next level. For matched subtables, update the corresponding beads of current level to eliminate the “u” values. This process is illustrated in Example 3.

Example 3. Assume that a MaxSAT model finds the truth table β 00010111 with the feature ordering $[f_1, f_2, f_3]$, and assume that the updated truth table β' is u0u1011u after phase (1). For level 1, we create a root node for β' as it is a bead. Then, we check the subtables of β' (u0u1 and 011u). Since they do not match, we move to the next level. For level 2, we create a node for u0u1 and a node for 011u as they are beads. Then, we check all subtables of the next level, which are u0, u1, 01 and 1u. We observe that u0 matches 1u, and u1 matches 01, therefore, the beads u0u1 and 011u are updated as 1001 and 0110. Therefore, the updated beads of β' are $\{u0u1011u, 1001(u0u1), 0110(011u), 10, 01, 0, 1\}$.

Figure 5 shows the beads updated (in the left), the BDD before the merging process (in the right) and the final BDD found (in the middle).

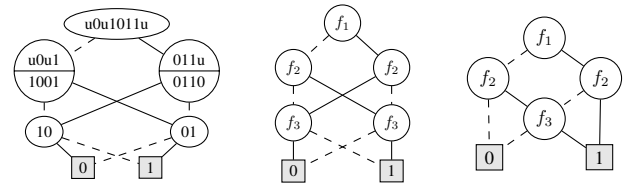


Figure 5: The BDD after merging compatible subtrees (the middle one) and the BDD before merging (the right one).

4 Experimental Results

We present our large experimental studies to evaluate empirically our propositions on different levels². At first, we make some preliminary experiments on the proposed SAT models to confirm the great improvements in the encoding size of BDD2 compared to BDD1, as shown theoretically in proposition 2 and 3. Then, we evaluate the prediction performance between the proposed MaxSAT-BDD model and the heuristic methods, ODT and OODG (Kohavi and Li 1995). Next, we compare our MaxSAT-BDD model with an exact method for building decision trees using MaxSAT (Hu et al. 2020) in terms of prediction quality, model size, and encoding size. Finally, we propose and evaluate a simple, yet efficient, scalable heuristic version of our MaxSAT-BDD model.

We consider datasets from CP4IM³. These datasets are binarized with the one-hot encoding. Table 3 describes the characteristics of these datasets: M indicates the number of examples, K_{orig} indicates the original number of features, K indicates the number of binary features after binarization, and pos indicates the percentage of positive examples.

All experiments were run on a cluster using Xeon E5-2695 v3@2.30GHz CPU running xUbuntu 16.04.6 LTS. The SAT solver we used is Kissat (Biere et al. 2020), the winner of SAT competition 2020. For each experiment of SAT encoding, we set 20 hours as the global timeout for SAT solver. The MaxSAT solver we used is Loandra (Berg, Demirović, and Stuckey 2019), an efficient incomplete MaxSAT solver. For each experiment of MaxSAT-BDD, the time limit for generating formulas and the time limit for solver are set to 15 minutes.

Dataset	M	K_{orig}	K	pos
anneal	812	42	89	0.77
audiology	216	67	146	0.26
australian	653	51	124	0.55
cancer	683	9	89	0.35
car	1728	6	21	0.30
cleveland	296	45	95	0.54
hypothyroid	3247	43	86	0.91
kr-vs-kp	3196	36	73	0.52
lymph	148	27	68	0.55
mushroom	8124	21	112	0.52
tumor	336	15	31	0.24
soybean	630	16	50	0.15
splice-1	3190	60	287	0.52
tic-tac-toe	958	9	27	0.65
vote	435	16	48	0.61

Table 3: Detailed Information Regarding the Datasets

Comparison Of The SAT Encodings

We consider the optimisation problem of finding a BDD that classifies all training examples correctly with the minimum depth. We use a simple linear search by solving multiple times the decision problem asking to find a BDD with a given

depth H (Problem $P_{bdd}(\mathcal{E}, H)$ in Section 3). We set the initial depth $H_0 = 7$. Considering the scalability problem, for each dataset, we use the hold-out method to split the training and testing set. We choose 5 different small splitting ratios $r = \{0.05, 0.1, 0.15, 0.2, 0.25\}$ to generate the training set. The remaining instances are used for testing. This process is repeated 10 times with different random seeds.

Table 4 reports the average results of instances that are solved to optimality by all methods within the given time. The columns “Acc” and “dopt” indicate the average testing accuracy in percent and the average optimal depth, respectively. The encoding size is given in column “E_Size” (i.e., the number of literals in the cnf file divided by 10^3). The column “Time” indicates the runtime in seconds of successful runs. The value “N/A” indicates the lack of results because of the timeout. The best values are indicated in blue.

Table 4 shows the great improvements in terms of the encoding size and the runtime of BDD2 compared to BDD1. This empirical observation is coherent with the complexity analysis made in Proposition 2 and 3. We also observe no substantial difference in terms of testing accuracy between the two approaches.

Datasets	ratio	BDD1				BDD2			
		Acc	dopt	E_Size	Time	Acc	dopt	E_Size	Time
anneal	0.05	N/A	N/A	N/A	N/A	68.65	6.33	9.43	192.74
audiology	0.05	75.99	2	0.83	0.46	76.86	2	0.83	0.07
	0.10	91.22	2.50	2.86	0.84	90.97	2.50	2.01	0.07
	0.15	92.54	2.80	5.37	1.39	93.3	2.80	3.26	0.09
	0.20	90.46	3.10	11.54	4.65	90	3.10	4.7	0.17
	0.25	92.94	3.60	23.53	31.79	92.45	3.60	6.81	0.39
australian	0.05	80.21	3.30	8.54	21.65	79.02	3.30	3.36	0.54
	0.10	N/A	N/A	N/A	N/A	77.46	6.22	15.21	7473.32
cancer	0.05	86.97	2.70	3.55	0.49	86.69	2.70	2.04	0.08
	0.10	89.97	4	23.15	4.95	89.24	4	6.01	0.55
	0.15	90.7	5.20	104.81	156.32	90.29	5.20	12.93	3.72
	0.20	91.53	6.40	390.71	10224.45	91.57	6.40	26.5	55.2
	0.25	N/A	N/A	N/A	N/A	92.16	6.44	35.12	200.12
car	0.05	76.81	7.62	162.38	5538.01	80.18	7.62	19.42	1924.9
cleveland	0.05	68.19	2.50	1.41	0.86	64.72	2.50	1.03	0.07
	0.10	68.58	3.80	9.15	121.11	69.29	3.80	2.94	0.92
	0.15	72.53	4.80	27.65	800.35	70.83	4.80	5.63	15.07
	0.20	N/A	N/A	N/A	N/A	68.78	6.10	10.9	2616.23
	0.25	N/A	N/A	N/A	N/A	68.74	6.90	18.13	16405.46
hypothyroid	0.05	96.26	5	131.80	319.09	96.3	5	18.22	2.98
lymph	0.05	67.23	2	0.33	0.13	68.79	2	0.34	0.07
	0.10	67.69	2.60	1.11	0.46	70.37	2.60	0.79	0.07
	0.15	70.16	3.40	3.41	2.83	71.98	3.40	1.52	0.16
	0.20	70.34	3.90	6.98	21.77	72.94	3.90	2.24	0.62
	0.25	72.23	5.10	23.08	410.10	68.48	5.10	3.91	4.31
mushroom	0.05	99.55	5.30	518.03	3774.19	99.48	5.30	60.03	28.32
	0.10	99.81	5.80	1523.69	12552.47	99.87	5.80	138.73	116.07
	0.15	99.87	5.90	2475.01	20616.09	99.86	5.90	213.62	210.98
	0.20	99.97	6	3503.87	29342.71	99.92	6	292.25	278.23
	0.25	99.96	6	4381.69	33787.52	99.95	6	365.18	437.4
soybean	0.05	80.52	3.90	5.74	2.94	78.58	3.90	1.78	0.21
	0.10	84.47	5.90	70.84	1391.79	82.22	5.90	7.48	7.46
tic-tac-toe	0.05	64.46	5.90	23.57	41.18	66.37	5.90	3.83	5.62
	0.10	72.68	7.60	206.10	18589.30	74.61	7.60	21.52	2846.24
vote	0.05	90.89	2.10	0.61	0.27	91.09	2.10	0.57	0.08
	0.10	91.93	2.60	1.99	0.57	91.63	2.60	1.34	0.08
	0.15	92.27	3.40	6.97	1.20	92.27	3.40	2.75	0.16
	0.20	92.35	4.10	20.68	26.43	92.44	4.10	4.76	0.71
	0.25	93	4.90	53.92	348.56	92.42	4.90	8.13	3.4

Table 4: Evaluation of the Reduced SAT Model

²The source code and datasets are available online at <https://gitlab.laas.fr/hhu/bddencoding>

³<https://dtai.cs.kuleuven.be/CP4IM/datasets/>

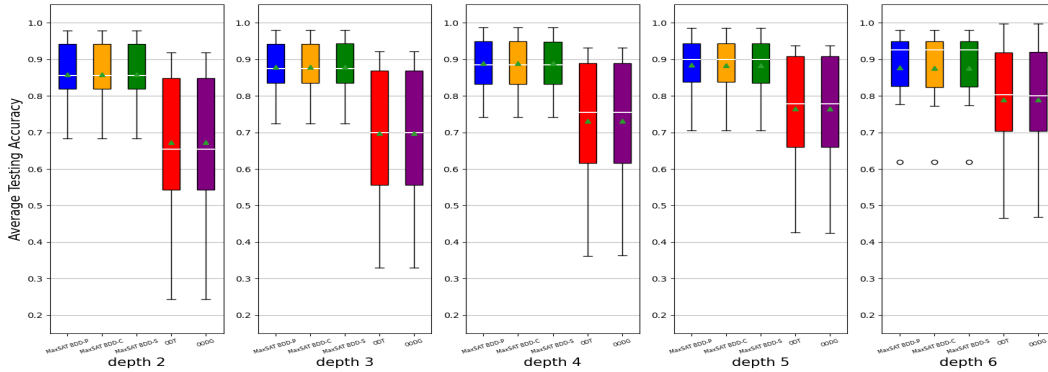


Figure 6: The average testing accuracy with different biases: **MaxSAT BDD-P**, **MaxSAT BDD-C**, **MaxSAT BDD-S**, ODT, OODG (respectively from left to right).

Comparison with Existing Heuristic Approaches

We consider the proposed MaxSAT-BDD model for solving the $P_{bdd}^*(\mathcal{E}, H)$ problem (defined in Section 3) with 5 different depths $H \in \{2, 3, 4, 5, 6\}$. For each dataset, we use random 5-fold cross-validation with 5 different seeds. We compare our MaxSAT-BDD model with the heuristic approaches proposed in (Kohavi and Li 1995) to learn ODT and OODG. For the heuristic methods, as described in the background section, after merging the *isomorphic* and *compatible* subtrees of ODT, the OODG changes the bias for those “unknown” nodes. In fact, different bias affects the prediction for unseen examples, but *not* for the training examples. Therefore, the training accuracies of ODT and OODG are equal whereas the testing accuracies could be different. This fact is also true in the MaxSAT-BDD model. In this experiment, we consider the following three biases:

- By assigning for each unknown node the majority class of its branch (denoted as **MaxSAT BDD-P**)
- By merging compatible subtrees (**MaxSAT BDD-C**)
- By using the class decided by the MaxSAT solver (**MaxSAT BDD-S**).

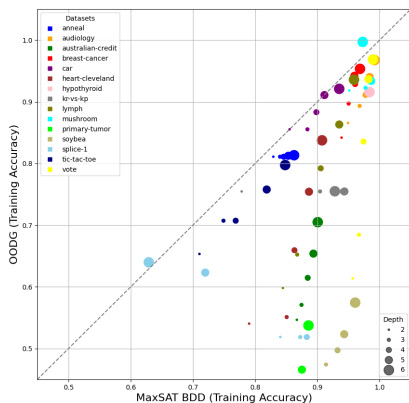


Figure 7: Comparison between the average training accuracy of OODG and the MaxSAT-BDD

Figure 7 presents the comparison of the average training accuracy between OODG and MaxSAT-BDD model. In this figure, different datasets are marked with different colors, and different depths are labelled with points of different sizes. From the scatter plot, we observe that the average training accuracy of both approaches increase with the increase of depth. Moreover, and more importantly, the MaxSAT-BDD model performs better than the heuristic OODG in training accuracy.

Figure 6 shows the average testing accuracy of MaxSAT-BDD with different biases, ODT, and OODG using different depths averaged over all datasets. The white line and green triangle of each box indicate the median and the average value, respectively. Clearly, the MaxSAT-BDD models have better prediction performance than ODT and OODG. This is particularly true with small depths. Increasing the depth increases the predictions for all methods as expected. However, the increase is less important with the different MaxSAT-BDD models. We observe also that there is little difference between the different biases for MaxSAT-BDD. This suggests that the optimal solutions are somewhat robust to the bias. We noticed also that for all datasets (except one), all MaxSAT-BDD models report optimality when the depth is equal to 2.

Comparison with an Exact Decision Tree Approach

The purpose of this experiment is to compare our proposition with the exact method for learning decision trees using the same solving approach (MaxSAT). For MaxSAT-BDD, we consider only the bias of merging compatible subtrees **MaxSAT BDD-C** since no substantial difference was observed between the different biases. We consider different values for the depth: $H \in \{2, 3, 4, 5, 6\}$. For each dataset, we use random 5-fold cross-validation with 5 different seeds. For MaxSAT-BDD, the depth also corresponds to the number of selected features, whereas for MaxSAT-DT the depth indicates the *maximum depth* of the BDD. Table 5 presents the results of the evaluation. The column “Size” and “E.Size” indicate the number of nodes of the model and the encoding size (number of literals divided by 10^3), respectively. The column “F.d” indicates the average number

of features used in the decision tree. The best values are indicated in blue.

The results in Table 5 show that the MaxSAT-BDD approach is competitive to MaxSAT-DT in terms of prediction quality. In most cases, the training and testing accuracy of these two approaches are close. However, the size of the models are always smaller with MaxSAT-BDD. The difference grows bigger when the depth increases. The reduction in model size provides better interpretability. Moreover, sometimes, compared to the optimal BDDs found via MaxSAT-BDD, the optimal decision trees found via MaxSAT-DT uses useless splits. This is, for instance, the case for the datasets “*car*” and “*hypothyroid*” with depth 2. We observe also that MaxSAT-BDD has always a much lighter encoding size than MaxSAT-DT. This gives a clear advantage to MaxSAT-BDD to handle the problem and to report optimality.

Evaluation of a Heuristic MaxSAT-BDD method

To increase the scalability of our model, we propose a simple heuristic version of MaxSAT-BDD. The idea is to perform as a pre-processing step to choose a subset of (important) features that are used exclusively in the MaxSAT-BDD model. By doing this, the search space is greatly reduced by focusing only on the selected features. We chose to run CART (Breiman et al. 1984) (an efficient and scalable heuristic for learning decision trees) to build quickly a decision tree. The features selected in our heuristic method are the ones used in the decision tree found by CART.

This experimental study follows the same protocol as the previous one. The results are detailed in Figure 8 and in Table 6.

As expected, the size of the encoding of the model is in favor of the heuristic approach. This is shown in the two columns **E.size** of Table 6. This advantage gives our approach the key to handle larger problems. Column **Opt** of Table 6 indicates the percentage of instances solved to optimality. It should be noted that proving optimality is much easier with the heuristic approach since the problem is naturally easier to solve with fewer features.

The results of the average testing accuracy are shown in the left scatter of Figure 8. Our heuristic approach is clearly very competitive to the exact MaxSAT-BDD in terms of learning generalization. This is particularly true for datasets with a large number of features. Indeed, the proposed heuristic approach obtains better prediction performance than the exact one within the same limited resources (time and memory). The middle and right scatters of Figure 8 show the comparison of the average training and testing accuracy between the heuristic approach and CART. It is clear that CART almost always gets better training accuracy. However, the heuristic MaxSAT-BDD is still competitive in terms of generalisation.

5 Conclusion

We propose exact and heuristic methods for optimizing binary decision diagrams (BDDs) based on the (Maximum) Boolean Satisfiability framework. Our large experimental

Datasets	H	MaxSAT BDD-C				MaxSAT-DT				
		Train	Test	Size	E.Size	Train	Test	Size	E.Size	F.d
anneal	2	82.92	82.19	5	24.09	83.18	82.14	6.84	52.72	2.88
	3	84	83.55	7	37.21	85.07	84.66	12.68	126.18	5.76
	4	84.58	83.84	9.4	52.06	86.05	84.78	18.68	315.45	8.64
	5	85.33	83.92	11.72	71.08	86.44	84.88	23.88	865.26	11.08
	6	86.26	83.70	14.68	99.47	87.6	85.76	39.16	2666.67	17.32
	audiology	2	94.91	94.92	4	10.59	95.49	94.92	7	31.35
3		96.78	95.84	5.04	16.41	97.82	95.56	11.56	88.75	5.28
4		97.73	95.56	6.96	22.56	99.51	94.54	19.08	272.15	8.68
5		98.40	94.44	9.88	29.82	99.95	93.98	27	915.29	11.72
6		99.17	95.84	14.28	39.59	99.86	94.08	24.12	3323.61	10.88
australian		2	86.70	85.94	4.72	26.79	86.93	85.33	6.68	59.65
	3	87.45	84.81	5.32	41.15	88.09	84.87	13.08	146.15	5.68
	4	88.45	86.03	7.4	56.85	88.74	85.18	17.48	377.62	7.92
	5	89.36	85.91	10.44	75.9	89.28	84.75	22.52	1076.35	10.08
	6	90.05	85.7	17.32	102.49	89.49	84.84	27.08	3433.64	12.20
	cancer	2	93.88	93.59	4	20.29	94.91	94.2	7	45.56
3		95.02	93.91	5.84	31.37	96.6	94.73	15	110.85	6.96
4		96.06	95.49	7.96	43.89	97.34	94.17	21	283.77	9.44
5		95.94	93.74	10.68	59.91	97.99	94.35	29.32	800.89	13.20
6		96.84	94.35	14.8	83.83	98.87	93.41	45.72	2536.91	19.88
car		2	85.53	85.53	4	13.32	85.53	85.53	6.84	32.01
	3	88.40	87.41	5.08	21.95	89.25	87.45	12.68	71.83	5.64
	4	89.84	88.54	6.84	34.44	91.62	89.68	20.36	162.46	7.68
	5	91.13	89.91	9.6	55.79	93.78	92.77	29.56	389.68	10.24
	6	93.51	92.99	13.36	97.06	95.8	95.06	31.96	1044.54	10.88
	cleveland	2	79.04	72.57	4	9.48	80.76	72.84	7	25.57
3		85.07	83.37	6	14.73	85.68	76.55	12.84	68.93	5.72
4		86.32	79.46	7.84	20.55	86.77	76.75	17.80	200.76	8.04
5		88.65	78.72	13.08	27.89	87.26	74.45	23.96	646.75	10.84
6		90.74	77.29	21.04	38.66	88.58	75.81	28.84	2284.76	13.08
hypothyroid		2	97.84	97.84	4	92.65	97.84	97.84	5.96	182.20
	3	98.09	98.04	5.12	142.78	98.14	97.82	9.72	402.98	4.32
	4	98.27	98.13	6.72	200.09	98.38	98.01	15.40	885.51	7.12
	5	98.30	98.05	9.28	274.03	98.45	98	20.04	2016.31	8.92
	6	98.37	97.95	13.68	385.4	98.46	97.91	33.16	4957.57	14.04
	kr-vs-kp	2	77.83	77.01	4	77.88	86.92	86.92	7	155.09
3		90.43	90.43	5.28	120.54	93.81	93.79	12.44	342.99	5.08
4		94.09	94.09	7.56	170.28	94.32	94.14	17.24	753.78	7.12
5		94.34	94.18	9.52	236.39	94.85	94.69	25.40	1717.14	10.20
6		92.80	92.55	11.52	339.35	93.91	93.69	29.32	4227.67	12.20
lymph		2	84.46	83.23	4	3.5	86.01	79.27	7	12.33
	3	86.76	78.35	5.92	5.55	91.93	80.54	14.68	36.65	6.64
	4	90.54	82.4	8.72	7.86	94.56	78.46	20.20	117.94	8.88
	5	93.51	83.6	13.52	10.94	97.09	82.46	27.08	413.09	11.88
	6	95.88	84.82	17.64	15.74	99.59	80.92	46.60	1550.34	18.96
	mushroom	2	95.13	95.13	4	299.19	96.9	96.9	7	565.27
3		97.74	97.77	6.8	458.1	99.9	99.9	13.72	1227.18	6.24
4		98.78	98.74	9	635.09	100	100	19.80	2603.94	9.08
5		98.63	98.57	11.32	853.68	100	100	23.40	5571.14	10.64
6		97.28	97.10	14.6	1165.88	100	100	27.56	12376.90	12.12
tumor		2	82.80	81.6	4	3.72	82.92	81.01	6.76	10.46
	3	83.84	80.43	5.3	6.02	86.16	82.97	13.88	27.24	6.08
	4	85.52	82.49	8.64	9.04	87.89	82.85	20.92	76.40	9.16
	5	87.51	85.83	13.32	13.79	90.1	79.34	47.80	239.09	16.84
	6	88.57	81.12	19.84	22.44	90.34	81.31	37.32	838.63	15.04
	soybean	2	90.48	90.48	4	10.79	91.27	91.27	7	25.55
3		91.39	90.41	6.52	16.99	95.45	94.7	15	62.30	7
4		93.24	93.21	9.04	24.54	97.25	95.9	22.20	160.18	9.88
5		94.31	92.95	11.92	35.34	97.96	95.3	40.60	455.33	15.72
6		96.07	95.52	14.88	53.41	98.27	96.03	33.40	1459.87	14.40
splice-1		2	84.04	84.04	4	296.61	84.22	83.17	6.92	555.22
	3	87.25	86.94	5.44	449.04	87.79	87.37	11.32	1231.59	4.64
	4	88.3	88.04	7.24	608.3	86.52	85.64	16.60	2717.90	7.12
	5	71.99	70.53	10.28	783.9	77.37	76.32	21.88	6226.75	9.48
	6	62.92	61.89	16.28	996.27	60.36	58.95	29.40	15406.05	12.28
	tic-tac-toe	2	71.05	68.35	4	9.25	71.1	67.49	5.96	22.31
3		74.91	72.36	6.16	15.01	77.15	73.55	11.48	51.98	5.20
4		76.87	74.22	8.84	22.88	82.47	78.68	20.60	125.10	8.44
5		81.86	80.31	13.88	35.67	83.08	79.50	28.44	328.33	11.16
6		84.82	80.08	24.16	59.52	84.25	80.86	38.12	979.46	13.24
vote		2	95.68	95.22	3.76	7.2	96.21	95.03	7	18.33
	3	96.69	94.57	5.56	11.38	97.39	93.79	13.96	46.55	6.04
	4	97.40	94.39	8.16	16.49	98.62	94.57	21.16	126.45	9.32
	5	98.21	94.57	12.4	23.83	99.47	93.84	30.52	381.95	12.96
	6	98.93	93.98	18.44	36.2	99.62	94.76	35.40	1292.44	14.88

Table 5: Comparison between MaxSAT-BDD and MaxSAT-DT.

studies show clear benefits of the proposed approach in terms of prediction quality and interpretability (compact topology) compared to the existing (heuristic) approaches.

In the future, it would be interesting to extend the proposed approach for multi-valued classification. Moreover, a

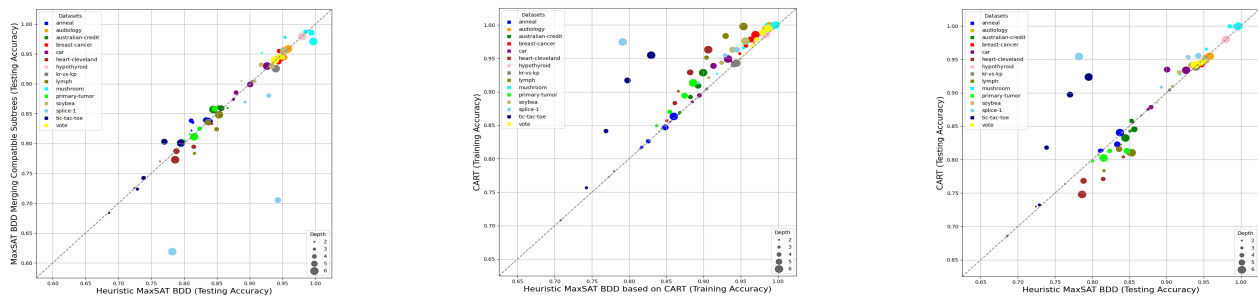


Figure 8: Left: comparison of Heuristic MaxSAT-BDD and Exact MaxSAT-BDD in testing accuracy. Middle: comparison of the training accuracy of Heuristic MaxSAT-BDD and CART. Right: comparison of the training accuracy of Heuristic MaxSAT-BDD and CART

deeper investigation of BDDs with other interpretable models (such as decision rules and decision sets) is needed for the sake of explainable AI.

References

- Aglin, G.; Nijssen, S.; and Schaus, P. 2020. Learning Optimal Decision Trees Using Caching Branch-and-Bound Search. In *The Thirty-Fourth AAAI Conference on Artificial Intelligence, AAAI 2020, The Thirty-Second Innovative Applications of Artificial Intelligence Conference, IAAI 2020, The Tenth AAAI Symposium on Educational Advances in Artificial Intelligence, EAAI 2020, New York, NY, USA, February 7-12, 2020*, 3146–3153. AAAI Press.
- Akers. 1978. Binary Decision Diagrams. *IEEE Transactions on Computers*, C-27(6): 509–516.
- Angelino, E.; Larus-Stone, N.; Alabi, D.; Seltzer, M.; and Rudin, C. 2018. Learning certifiably optimal rule lists for categorical data. *Journal of Machine Learning Research*, 18(234): 1–78.
- Avellaneda, F. 2020. Efficient Inference of Optimal Decision Trees. In *Proceedings of the Thirty-Fourth Conference on Artificial Intelligence (AAAI)*. New York, USA.
- Berg, J.; Demirović, E.; and Stuckey, P. J. 2019. Core-Boosted Linear Search for Incomplete MaxSAT. In *Proceedings of the 16th International Conference on the Integration of Constraint Programming, Artificial Intelligence, and Operations Research - CPAIOR*, 39–56.
- Bessiere, C.; Hebrard, E.; and O’Sullivan, B. 2009. Minimising Decision Tree Size as Combinatorial Optimisation. In *CP*, 173–187.
- Biere, A.; Fazekas, K.; Fleury, M.; and Heisinger, M. 2020. CaDiCaL, Kissat, Paracooba, Plingeling and Treengeling Entering the SAT Competition 2020. In *Proc. of SAT Competition 2020 – Solver and Benchmark Descriptions*, 49. To appear.
- Biere, A.; Heule, M.; van Maaren, H.; and Walsh, T., eds. 2009. *Handbook of Satisfiability*, volume 185 of *Frontiers in Artificial Intelligence and Applications*. ISBN 978-1-58603-929-5.
- Bonfietti, A.; Lombardi, M.; and Milano, M. 2015. Embedding Decision Trees and Random Forests in Constraint Programming. In Michel, L., ed., *Integration of AI and OR Techniques in Constraint Programming*, 74–90. Cham: Springer International Publishing. ISBN 978-3-319-18008-3.
- Breiman, L.; Friedman, J. H.; Olshen, R. A.; and Stone, C. J. 1984. *Classification and Regression Trees*. Chapman & Hall/CRC, 1st edition. ISBN 0-534-98053-8.
- Bryant, R. E. 1986. Graph-Based Algorithms for Boolean Function Manipulation. *IEEE Trans. Computers*, 35(8): 677–691.
- Cabodi, G.; Camurati, P. E.; Ignatiev, A.; Marques-Silva, J.; Palena, M.; and Pasini, P. 2021. Optimizing Binary Decision Diagrams for Interpretable Machine Learning Classification. In *Design, Automation & Test in Europe Conference & Exhibition, DATE 2021, Grenoble, France, February 1-5, 2021*, 1122–1125. IEEE.
- Clark, P.; and Boswell, R. 1991. Rule induction with CN2: Some recent improvements. In Kodratoff, Y., ed., *Machine Learning — EWSL-91*, 151–163. Berlin, Heidelberg: Springer Berlin Heidelberg. ISBN 978-3-540-46308-5.
- Cohen, W. W. 1995. Fast Effective Rule Induction. In Friedtits, A.; and Russell, S. J., eds., *Machine Learning, Proceedings of the Twelfth International Conference on Machine Learning, Tahoe City, California, USA, July 9-12, 1995*, 115–123. Morgan Kaufmann.
- Cover, T. M.; and Thomas, J. A. 2006. *Elements of Information Theory (Wiley Series in Telecommunications and Signal Processing)*. USA: Wiley-Interscience. ISBN 0471241954.
- Hu, H.; Huguet, M.-J.; and Siala, M. 2022. Optimizing Binary Decision Diagrams with MaxSAT for classification. In *Thirty-Sixth AAAI Conference on Artificial Intelligence, AAAI 2022, Virtual Event, February 22, March 1, 2022*. AAAI Press.
- Hu, H.; Siala, M.; Hebrard, E.; and Huguet, M. 2020. Learning Optimal Decision Trees with MaxSAT and its Integration in AdaBoost. In Bessiere, C., ed., *Proceedings of the Twenty-Ninth International Joint Conference on Artificial Intelligence, IJCAI 2020*, 1170–1176. ijcai.org.
- Ignatov, D. Y.; and Ignatov, A. D. 2017. Decision Stream: Cultivating Deep Decision Trees. In *29th IEEE International Conference on Tools with Artificial Intelligence, IC-*

Datasets	d	CART				Heuristic MaxSAT-BDD						MaxSAT-BDD					
		Train	Test	Size	F_d	Opt	Train	Test	Size	E_size	Time	Opt	Train	Test	Size	E_size	Time
anneal	2	81.53	81.21	6.12	2.56	100	81.53	81.13	3.56	1.45	0.13	100	82.92	82.19	5	24.09	92.93
	3	81.72	81.38	11.08	4.92	100	81.71	81.33	5.24	4.03	1.64	0	84	83.55	7	37.21	TO
	4	82.60	81.33	18.04	8.40	100	82.57	81.08	7.08	9.64	109.65	0	84.58	83.84	9.40	52.06	TO
	5	84.69	82.29	27.88	12.32	12	84.86	83.37	11.12	20.62	780.08	0	85.33	83.92	11.72	71.08	TO
	6	86.32	84.04	39.80	17	0	86.01	83.74	13.56	42.6	845.72	0	86.26	83.70	14.68	99.47	TO
	2	94.91	94.92	5	2	100	94.91	94.92	4	0.35	0.01	100	94.91	94.92	4	10.59	0.46
audiology	3	97.36	94.82	9	4	100	96.78	95.38	5.04	1	0.02	100	96.78	95.84	5.04	16.41	6.63
	4	98.73	95.37	13.08	6	100	97.73	95.56	7.04	2.27	0.08	100	97.73	95.56	6.96	22.56	56.31
	5	99.42	95.28	17.08	8	100	98.31	95.28	9.76	4.8	0.49	72	98.40	94.44	9.88	29.82	578.99
	6	99.88	95.47	19.08	9	100	98.87	95.84	13	9.78	2.13	48	99.17	95.84	14.28	39.59	613.06
	2	86.68	86.62	7	3	100	86.68	86.62	4.92	1.26	0.09	100	86.7	85.94	4.72	26.79	167.99
	3	86.91	84.26	13.08	6	100	86.83	85.09	5.48	3.59	2.41	0	87.45	84.81	5.32	41.15	TO
australian	4	89.23	85.79	24.92	11.84	84	88.24	85.30	6.8	9.22	536.16	0	88.45	86.03	7.40	56.85	TO
	5	90.9	84.53	41.64	19.24	0	89.27	85.67	10.64	20.28	845.28	0	89.36	85.91	10.44	75.90	TO
	6	92.86	83.24	64.28	28.84	0	89.95	84.47	16.12	41.85	TO	0	90.05	85.7	17.32	102.49	TO
	2	94.5	93.91	7	3	100	93.81	93.59	4	1.32	0.06	100	93.88	93.59	4	20.29	5.89
	3	95.7	94.41	13.24	6.08	100	94.89	94.14	5.64	3.78	0.52	100	95.02	93.91	5.84	31.37	525.59
	4	96.91	94.26	21.08	9.88	100	95.71	94.50	7.8	8.77	20.44	0	96.06	95.49	7.96	43.89	TO
cancer	5	97.83	94.20	30.36	14.04	60	96.35	94.35	10.92	18.32	637.98	0	95.94	93.74	10.68	59.91	TO
	6	98.54	94.38	38.84	17.68	0	96.98	94.67	15.20	36.33	864.36	0	96.84	94.35	14.8	83.83	TO
	2	85.53	85.53	5	2	100	85.53	85.53	4	2.77	0.14	100	85.53	85.53	4	13.32	24.82
	3	88.5	87.53	7	3	100	88.5	87.53	5	6.94	0.74	8	88.40	87.41	5.08	21.95	TO
	4	89.46	87.86	11	5	100	89.45	87.93	6.4	16.64	14.83	0	89.84	88.54	6.84	34.44	TO
	5	93.88	93.47	18.20	7.80	24	91.34	90.08	9.24	37.43	843.14	0	91.13	89.91	9.60	55.79	TO
car	6	94.99	93.37	28.68	10.32	0	93.30	92.65	11.76	79.23	TO	0	93.51	92.99	13.36	97.06	TO
	2	78.13	72.97	7	2.72	100	77.99	72.43	3.76	0.55	0.04	100	79.04	72.57	4	9.48	83.84
	3	85.68	80.41	15	6.24	100	85.07	84.2	6	1.68	2.28	0	85.07	83.37	6	14.73	TO
	4	88.31	77.09	29.96	13	24	86.15	81.49	7.6	4.46	811.89	0	86.32	79.46	7.84	20.55	TO
	5	92.9	76.82	49.88	21.36	0	88.21	78.84	13.24	9.82	862.94	0	88.65	78.72	13.08	27.89	TO
	6	96.3	74.79	67.80	28.92	0	90.64	78.64	20.2	19.2	TO	0	90.74	77.29	21.04	38.66	TO
hypothyroid	2	97.84	97.84	6.92	2.96	100	97.84	97.84	4	6.2	0.43	100	97.84	97.84	4	92.65	77.76
	3	98.13	97.86	12.84	5.52	100	98.09	97.99	5.16	16.95	4.62	0	98.09	98.04	5.12	142.78	TO
	4	98.39	98.15	22.04	9.80	100	98.28	98.2	6.56	41.23	262.45	0	98.27	98.13	6.72	200.09	TO
	5	98.48	98.04	31.72	14.24	0	98.32	98.07	8.84	87.02	TO	0	98.30	98.05	9.28	274.03	TO
	6	98.6	97.99	43.56	18.92	0	98.37	97.99	13.32	175.62	TO	0	98.37	97.95	13.68	385.40	TO
	2	77.30	76.35	5	2	100	77.30	76.35	4	5.12	0.55	0	77.83	77.01	4	77.88	TO
kr-vs-kp	3	90.43	90.43	8.44	3.72	100	90.43	90.43	5.40	13.92	5.77	0	90.43	90.43	5.28	120.54	TO
	4	94.09	94.09	13.88	6.44	100	94.09	94.09	7.68	33.69	56.23	0	94.09	94.09	7.56	170.28	TO
	5	94.09	94.09	21.88	9.96	20	94.09	94.09	8.48	74.68	795.33	0	94.34	94.18	9.52	236.39	TO
	6	94.29	93.87	31.32	14.04	0	94.42	93.97	11.80	157.84	846.3	0	92.80	92.55	11.52	339.35	TO
	2	84.53	82.25	7	3	100	84.39	83.89	4	0.29	0.01	100	84.46	83.23	4	3.50	2.84
	3	90.07	78.34	14.92	6.52	100	86.62	81.59	6	0.88	0.29	32	86.76	78.35	5.92	5.55	829.42
lymph	4	95.1	80.91	25.80	11.76	100	90.40	84.97	8.36	2.16	17.38	0	90.54	82.40	8.72	7.86	TO
	5	98.34	81.58	33.40	14.96	88	92.97	83.62	12.88	4.21	277.57	0	93.51	83.60	13.52	10.94	TO
	6	99.76	81.02	36.76	15.76	40	95.37	85.33	17.64	7.78	626.2	0	95.88	84.82	17.64	15.74	TO
	2	92.71	92.71	7	3	100	91.83	91.83	4	15.61	6.82	100	95.13	95.13	4	299.19	425.74
	3	96.56	96.54	11	5	100	95.37	95.37	5.8	40.33	23.11	0	97.74	97.77	6.80	458.10	TO
	4	99.95	99.94	16.92	7.96	100	98.52	98.52	8.24	93.45	89.39	0	98.78	98.74	9	635.09	TO
mushroom	5	99.96	99.94	18.92	8.96	96	99.41	99.41	11.12	183.13	458.08	0	98.63	98.57	11.32	853.68	TO
	6	99.97	99.96	20.92	9.76	4	99.70	99.69	13.32	367.46	821.83	4	97.28	97.10	14.60	1165.88	855.34
	2	82.77	80.65	7	3	100	82.75	80.83	4	0.66	0.05	100	82.8	81.6	4	3.72	5.46
	3	84.94	79.76	15	6.72	100	83.71	80.06	5.56	1.99	3.11	0	83.84	80.43	5.3	6.02	TO
	4	87.01	81.30	28.68	11.96	76	85.46	82.38	8.48	4.82	510.07	0	85.52	82.49	8.64	9.04	TO
	5	89.42	81.31	48.20	17.52	0	87.47	84.69	13.12	10.06	TO	0	87.51	85.83	13.32	13.79	TO
soybean	6	91.34	80.24	68.60	21.04	0	88.60	81.54	20.52	19.12	TO	0	88.57	81.12	19.84	22.44	TO
	2	89.13	88.54	6.92	2.76	100	89.30	88.76	4	1.17	0.05	100	90.48	90.48	4	10.79	9.51
	3	92.11	90.95	13.08	5.60	100	90.71	90.79	5	3.34	1.22	68	91.39	90.41	6.52	16.99	706.39
	4	94.36	93.05	21	9.40	100	92.44	91.75	7.92	7.9	96.96	0	93.24	93.21	9.04	24.54	TO
	5	96.29	94.13	31.88	13.40	28	93.90	93.37	11.08	16.58	804.03	0	94.31	92.95	11.92	35.34	TO
	6	97.58	94.89	43.48	16.88	0	95.65	95.24	14.56	33.04	TO	0	96.07	95.52	14.88	53.41	TO
splice-1	2	84.04	84.04	7	3	100	84.04	84.04	4	6.13	4.06	0	84.04	84.04	4	296.61	TO
	3	91.34	90.85	15	6.20	100	89.31	89.31	5.32	17.7	67.13	0	87.25	86.94	5.44	449.04	TO
	4	95.44	95.34	28.52	10.60	4	92.92	92.92	7.36	42.15	841.79	0	88.30	88.04	7.24	608.30	TO
	5	96.29	95.52	46.92	17.20	0	94.48	94.29	9.68	93.08	TO	0	71.99	70.53	10.28	783.90	TO
	6	97.45	95.44	76.44	29.64	0	79.13	78.22	15.12	205.48	TO	0	62.92	61.89	16.28	996.27	TO
	2	70.80	68.58	7	2.96	100	70.80	68.58	3.76	1.84	0.65	100	71.05	68.35	4	9.25	48.01
tic-tac-toe	3	75.65	73.21	15	6.76	100	74.26	72.90	6.04	5.6	92.88	0	74.91	72.36	6.16	15.01	TO
	4	84.14	81.8	27	11.04	0	76.89	73.86	9.04	12.99	TO	0	76.87	74.22	8.84	22.88	TO
	5	91.7	89.73	43.72	16	0	79.79	77.02	14.24	27.15	TO	0	81.86	80.31	13.88	35.67	TO
	6																

- pretable Decision Sets: A Joint Framework for Description and Prediction. In Krishnapuram, B.; Shah, M.; Smola, A. J.; Aggarwal, C. C.; Shen, D.; and Rastogi, R., eds., *Proceedings of the 22nd ACM SIGKDD International Conference on Knowledge Discovery and Data Mining, San Francisco, CA, USA, August 13-17, 2016*, 1675–1684. ACM.
- Matheus, C. J.; and Rendell, L. A. 1989. Constructive Induction On Decision Trees. In Sridharan, N. S., ed., *Proceedings of the 11th International Joint Conference on Artificial Intelligence. Detroit, MI, USA, August 1989*, 645–650. Morgan Kaufmann.
- Moret, B. M. E. 1982. Decision Trees and Diagrams. *ACM Comput. Surv.*, 14(4): 593–623.
- Mues, C.; Baesens, B.; Files, C. M.; and Vanthienen, J. 2004. Decision Diagrams in Machine Learning: An Empirical Study on Real-Life Credit-Risk Data. In Blackwell, A. F.; Marriott, K.; and Shimojima, A., eds., *Diagrammatic Representation and Inference, Third International Conference, Diagrams 2004, Cambridge, UK, March 22-24, 2004, Proceedings*, volume 2980 of *Lecture Notes in Computer Science*, 395–397. Springer.
- Narodytska, N.; Ignatiev, A.; Pereira, F.; and Marques-Silva, J. 2018. Learning Optimal Decision Trees with SAT. In Lang, J., ed., *Proceedings of the Twenty-Seventh International Joint Conference on Artificial Intelligence, IJCAI 2018, July 13-19, 2018, Stockholm, Sweden*, 1362–1368. ijcai.org.
- Oliver, J. J. 1993. Decision Graphs - An Extension of Decision Trees.
- Pagallo, G.; and Haussler, D. 1990. Boolean Feature Discovery in Empirical Learning. *Mach. Learn.*, 5: 71–99.
- Quinlan, J. R. 1986. Induction of Decision Trees. *Machine Learning*, 1(1): 81–106.
- Quinlan, J. R. 1993. *C4.5: programs for machine learning*. Morgan Kaufmann Publishers Inc. ISBN 1-55860-238-0.
- Rokach, L.; and Maimon, O. 2014. *Data Mining With Decision Trees: Theory and Applications*. USA: World Scientific Publishing Co., Inc., 2nd edition. ISBN 9789814590075.
- Shannon, C. E. 1938. A symbolic analysis of relay and switching circuits. *Electrical Engineering*, 57(12): 713–723.
- Sinz, C. 2005. Towards an Optimal CNF Encoding of Boolean Cardinality Constraints. In van Beek, P., ed., *Principles and Practice of Constraint Programming - CP 2005, 11th International Conference, CP 2005, Sitges, Spain, October 1-5, 2005, Proceedings*, volume 3709 of *Lecture Notes in Computer Science*, 827–831. Springer.
- Verhaeghe, H.; Nijssen, S.; Pesant, G.; Quimper, C.; and Schaus, P. 2020. Learning optimal decision trees using constraint programming. *Constraints An Int. J.*, 25(3-4): 226–250.
- Verwer, S.; and Zhang, Y. 2019. Learning optimal classification trees using a binary linear program formulation. In *Proceedings of the Thirty-Third National on Artificial Intelligence, AAAI-19*, 1625–1632. AAAI Press.
- Voigt, P.; and Bussche, A. v. d. 2017. *The EU General Data Protection Regulation (GDPR): A Practical Guide*. Springer Publishing Company, Incorporated, 1st edition. ISBN 3319579584.
- Yu, J.; Ignatiev, A.; Stuckey, P. J.; and Bodic, P. L. 2020. Computing Optimal Decision Sets with SAT. In Simonis, H., ed., *Principles and Practice of Constraint Programming - 26th International Conference, CP 2020, Louvain-la-Neuve, Belgium, September 7-11, 2020, Proceedings*, volume 12333 of *Lecture Notes in Computer Science*, 952–970. Springer.

Appendix: Algorithm for Producing A BDD Based on the Beads of a Truth table

Recall that Proposition 1 states that there is a one-to-one correspondence between the vertices of a BDD and the beads of the correspondent Boolean function. Consider a string β of length 2^H associated to a sequence of variables $[x_1, x_2, \dots, x_H]$. This appendix describes the algorithm we used to construct a BDD of a maximum depth H using the beads of β .

As the BDD built is *ordered* and *reduced*, it contains no isomorphic subtrees. This algorithm creates nodes level by level in a *breadth-first* way.

The BDD constructed is defined by a *list of nodes* and a *list of edges*. Each node is a pair $(node_id, variable)$. The value of $node_id$ is a unique integer called the id of the node which is non-negative for non terminal nodes. There are two sink nodes: $(-1, 1)$ associated to the value 1 (i.e., positive class in the context of binary classification); and $(-2, 0)$ associated to for the value 0 (i.e., negative class in binary classification). Each edge is a tuple $(p, c, direction)$, where p is the id of the parent node, c is the if of the child, and $direction \in \{left, right\}$ indicates if c is the left or right child of p .

Before we present the algorithm, we show some predefined functions used in the algorithm in Table 7.

Function(Input): Output	Description
$FirstHalf(string\ s)$: string	Returns the first half of s
$SecondHalf(string\ s)$: string	Returns the second half of s
$IsBead(string\ s)$: Boolean	Returns <i>True</i> iff s is a bead
$LeadToZero(string\ s)$: Boolean	Returns <i>True</i> iff s contains only 0
$LeadToOne(string\ s)$: Boolean	Returns <i>True</i> iff s contains only 1

Table 7: Predefined functions in the algorithm

The detailed algorithm is described in Algorithm 1. We use a FIFO queue q in the algorithm. Each item in the queue follows the format $(str, parent_id, current_level, direction)$. The first item pushed in the queue is a special case associated to the root denoted by $(\beta, 0, 1, \emptyset)$ since the root has not parent.

At each iteration of the main loop, the algorithm pops an element $(s, parent_id, level, direction)$ from the queue at Line 6. If s is a bead, the algorithm creates a new node at Line 13 associated with the level $level$ if s is seen for the first time. The set of edges is updated in Line 17 accordingly. The left and right children of s are added in the queue in Lines 20 and 21.

When the current string s is not a Bead of size > 1 , there might be two cases where s leads immediately to a sink node. Either s contains only 0s or s contains only 1s. The two cases are handled (according to the size of s) in two parts of the algorithm: from Lines 22 to Line 36 and from Lines 42 to Line 48. The case where s is a bead that is not equivalent to a sink node, the set of edges is updated and only one child of s is added to the queue without creating nodes (since s is a bead). The algorithm ends when all the elements of the queue are treated.

Algorithm 1: GenBDD(β, \mathcal{X}), an algorithm to construct a BDD from a given string β and variable sequence \mathcal{X}

Input: String β , variable sequence $\mathcal{X} = [x_1, \dots, x_H]$.

Output: BDD($nodes, edges$)

```

1:  $nodes \leftarrow \{\}; edges \leftarrow \{\}; T \leftarrow \{\}$ 
2:  $nodes.append((-1, 1)); nodes.append((-2, 0))$ 
3:  $q \leftarrow Queue()$ 
4:  $q.put((\beta, 0, 1, \emptyset))$ 
5: while not  $q.empty()$  do
6:    $(s, parent\_id, level, direction) \leftarrow q.pop()$ 
7:   if  $Length(s) > 1$  and  $IsBead(s)$  then
8:     // When the current string  $s$  is a Bead.
9:     if  $s \notin T$  then
10:      //  $s$  is a new string, i.e., not seen before
11:       $T.append(s)$ 
12:       $index \leftarrow T.index(s) + 1$ 
13:       $nodes.append((index, x_{level}))$ 
14:    end if
15:     $index \leftarrow T.index(s) + 1$ 
16:    if  $parent\_id \geq 1$  then
17:       $edges.append((parent\_id, index, direction))$ 
18:    end if
19:    // Put the left and right child into the queue.
20:     $q.put((FirstHalf(s), index, level + 1, left))$ 
21:     $q.put((FirstHalf(s), index, level + 1, right))$ 
22:  else if  $Length(s) > 1$  and not  $IsBead(s)$  then
23:    // When the current string  $s$  is not a Bead.
24:    if  $LeadToOne(s)$  or  $LeadToZero(s)$  then
25:      //  $s$  leads to sink nodes
26:      if  $LeadToOne(s)$  then
27:         $sink \leftarrow -1$ 
28:      else
29:         $sink \leftarrow -2$ 
30:      end if
31:      if  $p = 0$  then
32:         $edges.append((1, sink, left))$ 
33:         $edges.append((1, sink, right))$ 
34:      else
35:         $edges.append((parent\_id, sink, direction))$ 
36:      end if
37:    else
38:      // Otherwise put the left child into the queue.
39:       $q.put((FirstHalf(s), parent\_id, level + 1, direction))$ 
40:    end if
41:  else
42:    // The current string is a sink node.
43:    if  $s = 1$  then
44:       $sink \leftarrow -1$ 
45:    else
46:       $sink \leftarrow -2$ 
47:    end if
48:     $edges.append((parent\_id, sink, direction))$ 
49:  end if
50: end while

```
